

# Characterization by electrochemical impedance spectroscopy of a dye-sensitized solar cell using a natural anthocyanin pigment extracted from *Sorghum* spp

Mahamadou Hamza Garba <sup>1</sup>, Abdoukadi Ayouba Mahamane <sup>1,\*</sup>, Abourahmane Saidou Boulhassane <sup>1</sup>, Moutari Souley Kallo <sup>2</sup>, Hassane Adamou Hassane <sup>1</sup>, Illyassou Karimoun Massalatchi <sup>2</sup> and Rabani Adamou <sup>1</sup>

<sup>1</sup> Department of Chemistry/Faculty of Science and Techniques/Abdou Moumouni University, P.O. Box 10662, Niamey, Niger

<sup>2</sup> Department of Chemistry/Ecole Normale Supérieure/Abdou Moumouni University, P.O. Box 10963, Niamey, Niger

**Abstract:** A natural dye solar cell is a low-cost, environmentally friendly device that converts sunlight into electricity. Charge transport, charge transfer, and charge recombination are the main processes in the dye-sensitized solar cell. However, these processes in these types of cells are still poorly understood. This work aims to characterize the natural dye-sensitized solar cell of *Sorghum* spp using electrochemical impedance spectroscopy. A liquid-liquid dye separation of an aqueous crude extract of *Sorghum* spp was carried out with four organic solvents of increasing polarity to identify the most effective extract. Dye-sensitized solar cells with an active surface area of 1 cm<sup>2</sup> were fabricated and characterized using the current density-voltage method and electrochemical impedance spectroscopy (EIS) under illumination of 1000 W.m<sup>-2</sup>. The energy conversion efficiency of the cells from the different extracts ranged from 0.13 to 0.19%. The electron recombination resistance at the TiO<sub>2</sub>/dye/electrolyte interface varied from 316.59 Ω to 532.27 Ω, and the electron lifetime in TiO<sub>2</sub> varied from 24.843 to 49.575 ms. Among the cells studied, those with dyes from dichloromethane (Dcm-Ex) and ethyl acetate (Ea-Ex) extracts had the best performance despite the high electron recombination, compensated by the longer electron lifetime observed in those cells.

**Keywords:** Dye-sensitized solar cell, *Sorghum* spp, natural dye, impedance techniques.

## 1. Introduction

In recent decades, abundant fossil fuels have enabled unprecedented industrial development. Nowadays, as it is acknowledged that global warming and climate change are primarily caused by the direct release of carbon dioxide and other greenhouse gases into the atmosphere from these energies <sup>1</sup>, there is a strong consensus towards using more renewables in the energy mix. These renewables include geothermal, wind, biomass, hydropower, and solar energies and would enable a clean and sustainable industrial and economic transition <sup>2</sup>. Among these energy sources, solar energy is the best because the sun is free, inexhaustible, and does not emit greenhouse gases. Photovoltaic solar energy is the technology that converts solar radiation into electricity. Different photovoltaic devices like inorganic, organic, and hybrid solar cells have been invented for several years using various applications. Moreover, the high conversion efficiency of silicon solar cells, the high cost of the module, and the complicated production processes involved in the production restrict the

commercialization of photovoltaic solar cells as a means of electricity supply. Among all organic solar cells, Dye-Sensitized Solar Cells (DSSCs), or Grätzel cells, developed in 1991, are the most efficient, low-cost, promising and easily implemented technology <sup>3</sup>. DSSCs are inspired by the natural photosynthesis of plants, in which the functions of light absorption and charge transfer are separated. A photosensitizer is responsible for absorbing light, while a semiconductor is responsible for transmitting and collecting it <sup>3</sup>. The pigment-sensitized solar cell has achieved a light-to-electricity conversion efficiency of around 14% with the ruthenium complex dye <sup>3</sup>.

More recently, solar cells based on lead halide perovskite, which has excellent optical and photoelectric properties, have achieved a record efficiency of 25.7% <sup>4</sup>, challenging monocrystalline silicon solar cells. However, the ruthenium and lead used in this cell type are unsuitable for mass production due to their high cost, limited availability, toxicity, and environmental impact <sup>4-6</sup>. In contrast to

\*Corresponding author: Abdoukadi Ayouba Mahamane

Email address: [kadayouba@gmail.com](mailto:kadayouba@gmail.com)

DOI: <http://dx.doi.org/10.13171/mjc02410141804mahamane>

Received August 8, 2024

Accepted September 30, 2024

Published October 14, 2024

synthetic dyes, natural dyes are inexpensive, non-toxic, biodegradable, environmentally friendly<sup>7</sup> and readily available<sup>8</sup>. For this reason, many natural organic dyes extracted from various plant species' leaves, fruits, and flowers have been actively studied and tested as a low-cost alternative to rare and expensive ruthenium-based dyes<sup>8</sup>. In a Grätzel cell, the dye plays a key role in converting light into electricity. However, the internal mechanism of the solar cell, such as the transport and diffusion process, the regeneration of electrons and carriers, and the recombination of electrons, has not been sufficiently investigated. The main objective of this work is to characterize a solar cell sensitized with a natural pigment found in the sheaths of *Sorghum* spp using electrochemical impedance spectroscopy better to understand the electronic exchanges in this type of cell.

## 2. Experimental

### 2.1. Samples

The plant material consists of the sheaths of *Sorghum* spp. In Niger, the plant is mainly used in

textiles and handicrafts, for example, in basketry to decorate mats in red, blue, pink or orange in certain regions. The use of *Sorghum* spp sheaths as a dye source in dye-based solar cells poses no environmental problems. This plant is cultivated in Niger and its sheaths are available in large quantities at an affordable cost<sup>9</sup>.

### 2.2. Extraction of dye from the sheaths of *Sorghum* spp

The *Sorghum* spp sheaths were washed with distilled water and then dried overnight in an oven set at 50 °C in the dark. After drying, the sheaths were crushed to a fine powder using a hand grinder. The dyes were extracted from the powder by maceration of 40 g of the sample in 200 mL of 70% ethanol for 24 h with stirring. This process was repeated three times to extract as much dye as possible. After decantation, filtration, and evaporation of the collected extracts, a dark red colored crude extract powder was obtained after drying in the shade without sunlight<sup>9</sup>. The crude dye extraction process is described in Figure 1.

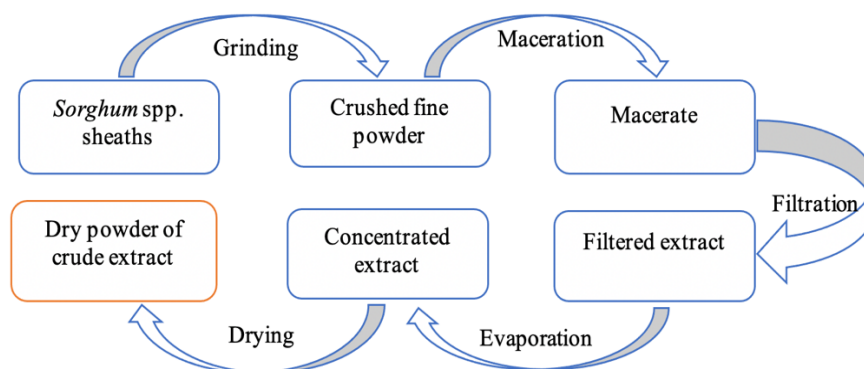


Figure 1. Simplified diagram of the dye extraction process.

### 2.3. Purification of the crude pigment

A mass of 0.5 g of crude *Sorghum* spp extract powder was weighed and dissolved in 50 mL of distilled water to give an aqueous solution of 10 g.L<sup>-1</sup>. For purification, the crude pigment was subjected to liquid-liquid separation. Thus, 50 mL of *Sorghum* spp dye was successfully confronted with 20 mL of organic solvents of increasing polarity, particularly petroleum ether, dichloromethane, ethyl acetate, and n-butanol. The aqueous crude extract of *Sorghum* spp and its colored organic extracts obtained by liquid-liquid separation were evaporated using a sand bath. After evaporation of the solvents, 15 mL of ethanol was added to each extract, which was then protected from light by aluminum foil and used as sensitizers<sup>9</sup>.

### 2.4. UV - Visible spectroscopy

The crude aqueous dye extract from *Sorghum* spp sheaths and its extracts from the liquid-liquid

separation were subjected to UV-visible analysis using an Evolution 300 UV-visible spectrophotometer. The absorbance in the visible region was determined by scanning the wavelength range from 400 to 800 nm.

### 2.5. Cyclic voltammetry

Cyclic voltammetry measurements were carried out on the different *Sorghum* spp extracts to determine the onset reduction potential<sup>9</sup>, using a potentiostat (Palm Sens4) connected to an electrochemical cell with three electrodes (including a glassy carbon working electrode, a silver chloride (Ag/AgCl, KCl<sub>sat</sub>) reference electrode and a platinum counter electrode). The 0.1 M KNO<sub>3</sub> solution was used as the supporting electrolyte. The scanning speed was 100 mV.s<sup>-1</sup> in the range -1000 mV to +1000 mV. The initial direction was positive, and the number of cycles was three (3).

## 2.6. Fourier Transform Infrared Spectroscopy (FT-IR)

Fourier Transform Infrared (FT-IR) spectrophotometer (Agilent) characterization was performed to determine the different functional groups present in the crude extract powder of *Sorghum* spp. Absorption spectrum was recorded between 4000 and 650  $\text{cm}^{-1}$ .

## 2.7. Electrodes preparation and solar cell assembly

The photoanode was prepared by applying a 1  $\text{cm}^2$  square pattern to the conductive side of the ITO glass slide using 3M tape. The  $\text{TiO}_2$  paste was deposited on this surface using the doctor blade method. After

the paste has dried, the tape was removed, and the film was sintered at 500  $^\circ\text{C}$ . After cooling, the  $\text{TiO}_2$  film electrode was immersed in the dye for 24 hours. The cathode was prepared by depositing a platinum solution on the conductive side of the ITO glass and then heated at 450  $^\circ\text{C}$  for 30 minutes on a hot plate. The cell is assembled by bringing the cathode against the anode platinum side against the dye side. Two clips were used on each side of the cell to hold the two electrodes together. One or two drops of the tetrabutylammonium iodide solution were applied to the edges of the slides using a syringe, alternately opening and closing the two clips to allow the electrolyte to penetrate <sup>9</sup>. Figure 2 shows the solar cell assembly process.

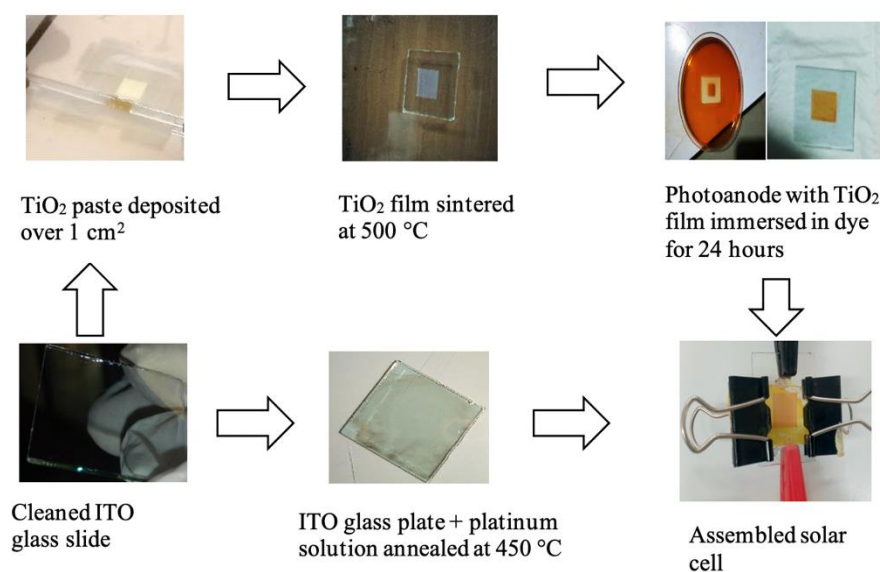


**Figure 2.** Dye-sensitised solar cell assembly process diagram.

## 2.8. Scanning Electron Microscopy (SEM) characterization

The surface morphology of a 1  $\text{cm}^2$   $\text{TiO}_2$  film heated at 500  $^\circ\text{C}$  with and without dye was characterized using a Scanning Electron Microscope Phenom PRO X.

## 2.9. Photoelectrochemical characterization

Cells with an active surface area of 1  $\text{cm}^2$  sensitized with natural dyes extracted from *Sorghum* spp were characterized under the illumination of 1000  $\text{W}\cdot\text{m}^{-2}$  emitted by a 50 W LED lamp in a circuit consisting of two multimeters and a variable resistor. A solarimeter was used to measure the incident light power. The recorded current density and corresponding voltage values were used to draw characteristic current density-voltage curves  $J = f(V)$ . Photovoltaic parameters such as open circuit voltage ( $V_{oc}$ ), short circuit current density ( $J_{sc}$ ), fill factor (FF), and energy conversion efficiency ( $\eta$ ) were derived from these curves <sup>8</sup>.

## 2.10. Electrochemical impedance spectroscopic measurement

The impedance measurements were performed to determine impedance parameters such as charge transfer resistances at the cell interfaces and electron lifetimes <sup>10</sup>. The electrochemical spectra were measured at an open-circuit solar cell with a potentiostat (Palm Sens4) by connecting the working and reference electrodes to the photoanode of the cell and the platinum electrode to the counter-electrode; this is equivalent to a two-electrodes measurement controlled by a computer equipped with a frequency response analyzer in the frequency range 0.05 to 100 kHz. The cell was placed under polarised illumination with a power of 1000  $\text{W}\cdot\text{m}^{-2}$  from a 50 W LED light source. The amplitude of the alternating signal was set to 10 mV. PS Trace 5.7 software was used to process the data, producing two types of plots, Nyquist and Bode.

### 3. Results and Discussion

#### 3.1. Extraction of *Sorghum* spp pigment and liquid-liquid separation of the aqueous crude extract solution (CAq-Ex)

A crude extract powder from *Sorghum* spp sheaths weighing 18.2 g was obtained after maceration of 120 g of finely ground sample, giving an extraction yield of 15.16%.

Following the liquid-liquid separation of the aqueous crude extract solution (CAq-Ex), other colored extracts were obtained (Figure 3), namely dichloromethane extract (Dcm Ex), ethyl acetate extract (Ea-Ex) and n-butanol extract (n-But-Ex). In contrast, the petroleum ether extract was colorless and did not separate any colored molecules.

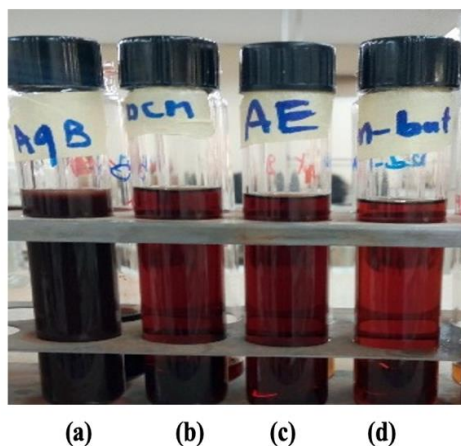


**Figure 3.** Natural dyes from *Sorghum* spp crude aqueous extract and colored organic extracts.  
(a): CAq-Ex, (b): Dcm-Ex, (c): Ea-Ex, (d): n-But-Ex

#### 3.2. UV-Visible Characterisation

The UV-Visible absorption spectra of various coloured extracts recorded at wavelengths between 400 nm and 800 nm are shown in Figure 4. In the

visible region, an absorption band is observed at a wavelength between 450 and 550 nm. This absorption could be attributed to the presence of anthocyanin molecules<sup>9</sup>.

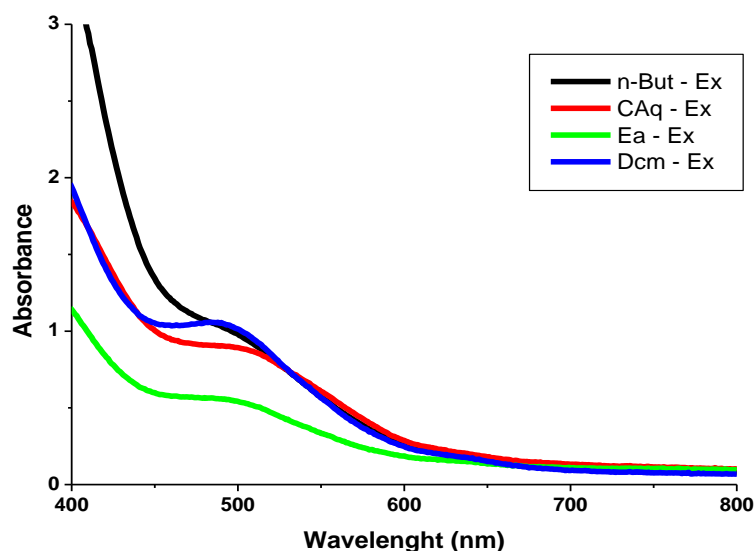


**Figure 4.** UV-visible spectra of extracts from the sheaths of *Sorghum* spp.

#### 3.3. Fourier Transform Infrared Spectroscopy

FT-IR spectrum of the dye from *Sorghum* spp crude extract is shown in Figure 5. A broadband visible at 3183  $\text{cm}^{-1}$  is characteristic of the stretching vibration of the phenolic OH hydroxyl group. A strong peak was observed at 1599  $\text{cm}^{-1}$ , followed by another at 1505, characteristic of the stretching vibration of the

aromatic C=C bond. The peak observed at 1226  $\text{cm}^{-1}$  could explain the stretching vibration of the C - O bond of the C - OH functions linked to the aromatic nucleus or the acid functions in the molecule. All these functional groups reveal the presence of anthocyanin molecules in the powder of *Sorghum* spp sheaths<sup>9, 11-12</sup>.

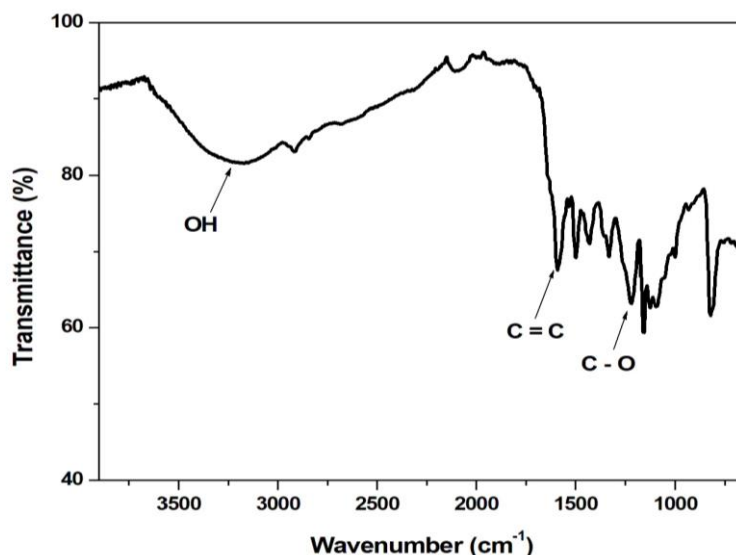


**Figure 5.** FT-IR spectrum of crude *Sorghum* spp sheets extracts dye.

### 3.4. Scanning Electron Microscopy (SEM)

The morphology of the photoanode  $\text{TiO}_2$  strongly affects the photoelectrochemical activity of the DSSCs. The SEM image (Figure 6 (a)) shows that the surface of  $\text{TiO}_2$  heated to  $500^\circ\text{C}$  has aggregated particles forming nanoclusters<sup>13</sup>. The pores appear open, which may facilitate the penetration of dye and

electrolyte. After adsorption of *Sorghum* spp sheath dye onto the  $\text{TiO}_2$  film (Figure 6 (b)), the aggregation of the  $\text{TiO}_2$  layer improved and a slight change in the spherical shape of the  $\text{TiO}_2$  particles was observed. This would be due to the adsorption of the dye molecules in the  $\text{TiO}_2$  layer.

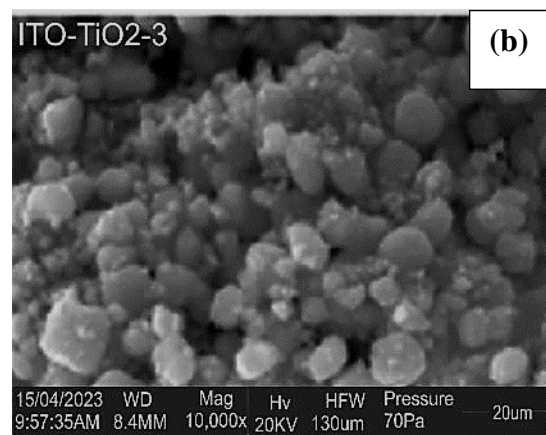
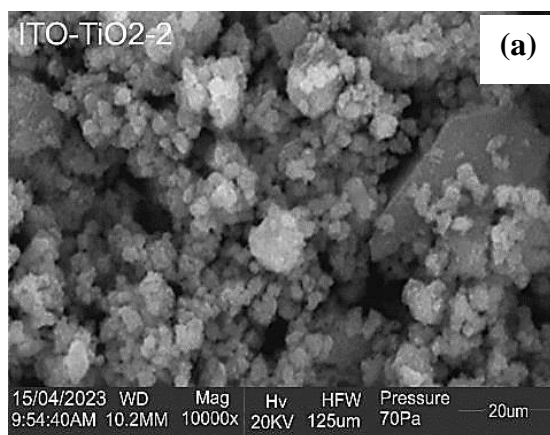


**Figure 6.** SEM images. (a):  $\text{TiO}_2$  heated at  $500^\circ\text{C}$ , (b):  $\text{TiO}_2$  heated at  $500^\circ\text{C}$  and immersed in the dye.

### 3.5. Photovoltaic Characteristics of DSSCs

The current density-voltage curves of the solar cells from the different extracts are plotted in Figure 7,

and the photovoltaic parameters extracted from the curves are listed in Table 1.

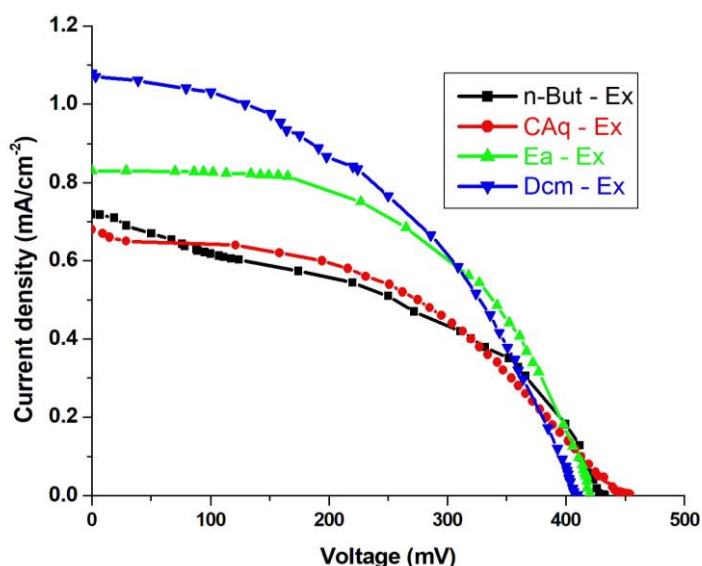


**Figure 7.** Current density-voltage (J-V) curves of cells sensitized with crude aqueous extract dye (CAq-Ex), dichloromethane extract dye (Dcm-Ex), ethyl acetate extract dye (Ea-Ex), and n-butanol extract dye (n-But-Ex).

**Table 1.** Photovoltaic parameters.

Extracts	$V_{oc}$ (mV)	$J_{sc}$ (mA.cm <sup>-2</sup> )	$P_{max}$ (mW cm <sup>-2</sup> )	FF	$\eta$ (%)
CAq-Ex	454	0.680	137.50	0.44	0.14
Dcm-Ex	412	1.079	190.84	0.43	0.19
Ea-Ex	420	0.830	181.06	0.52	0.18
n-But-Ex	432	0.719	130.77	0.42	0.13

The CAq-Ex dye-sensitized cell recorded a current density of 0.680 mA.cm<sup>-2</sup> and a conversion efficiency of 0.14%. After liquid-liquid separation, the current densities and conversion efficiencies for the solar cells sensitised with Dcm-Ex (1.079 mA.cm<sup>-2</sup>, 0.19%), Ea-Ex (0.830 mA.cm<sup>-2</sup>, 0.18%) and n-But-Ex dyes (0.719 mA.cm<sup>-2</sup>, 0.13%) were improved compared to those for the solar cell sensitized with CAq-Ex dye (0.680 mA.cm<sup>-2</sup>, 0.14%). These results would suggest that the separation had a purifying effect and reduced competition with the molecules present in the crude aqueous extract of *Sorghum* spp. This would be the basis for the improvement in conversion efficiency, which increased from 0.14% for the crude aqueous extract to 0.19% for the Dcm-Ex, i.e. a rate of improvement in efficiency of around 36%. It can also be noted that the extracts mainly composed of anthocyanin molecules from *Sorghum* spp that gave the best performance were derived from less polar solvents (dichloromethane and ethyl acetate). This would suggest that the most efficient anthocyanin molecules in the crude aqueous extract of *Sorghum* spp have a greater affinity for less polar solvents such as Dcm and Ea.

Furthermore, the low values of the open circuit voltages ( $V_{oc}$ ) observed for the sensitized cells by the dyes from the Dcm and Ea extracts (412 mV and 420 mV respectively), compared to those of the CAq-Ex

and n-But-Ex dyes (432 mV and 454 mV, respectively), are probably related to the good electron injection into the TiO<sub>2</sub> conduction band (CB) by the Dcm and Ea dyes. Good electron collection in the TiO<sub>2</sub> CB shifts the Fermi level towards negative potentials (relative to vacuum), hence the decrease in  $V_{oc}$ <sup>14</sup>. On the other hand, this good electron injection into the TiO<sub>2</sub> CB would also explain the relatively high current density in cells sensitized with Dcm-Ex and Ea-Ex dyes (1.079 mA.cm<sup>-2</sup> and 0.830 mA.cm<sup>-2</sup>, respectively). This relatively high current density compensates for the decrease in  $V_{oc}$ ; hence, the better performance of Dcm and Ea extracts sensitized cells compared to the others.

### 3.6. Energy gap determination, Cyclic voltammetry

The UV-visible absorption data and the Tauc relation were used to construct the curve whose equation is as follows<sup>9, 15-16</sup>:

$$(ah\nu)^2 = f(h\nu) \quad (1)$$

$a$  is the absorption coefficient,  $h\nu$  is the energy of a photon.

The absorption coefficient of a film of thickness  $d$  is calculated from the measurement of its absorbance  $A$  using the following relationship, where  $d$  is the optical path length:

$$a = 2.303 \times A/d \quad (2)$$

Each extract's energy gap ((E) was estimated by extrapolating the straightest part of the curve on the x-axis as shown in Figure 8.

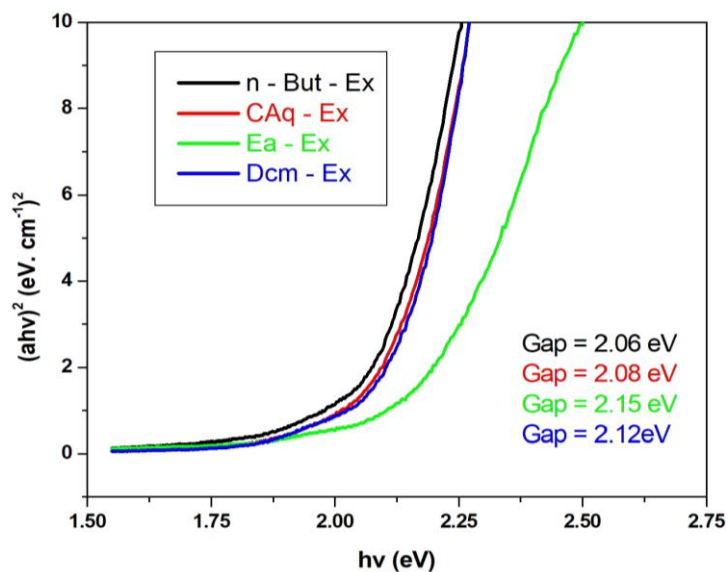


**Figure 8.** Determination of the energy gaps of the different extracts of *Sorghum* spp.

The reduction potential onset of the different extracts

determined from the voltammograms is shown in Figure 9.

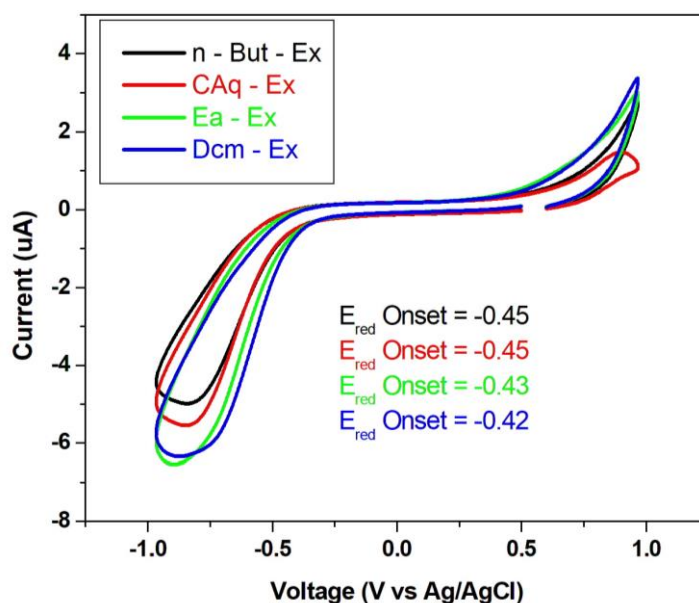


**Figure 9.** Cyclic voltammograms and reduction potentials onset of colored extracts.

The reduction potential onset of each dye was used to calculate the values of the highest occupied molecular orbital (HOMO) and the lowest unoccupied molecular orbital (LUMO) of each dye (Table 2) using the following relationships<sup>9, 17-19</sup>.

$$E_{(HOMO)} = -e[E_{ox}^{onset} + 4.4] \quad (4)$$

$$E_{(LUMO)} = -e[E_{red}^{onset} + 4.4] \quad (5)$$

$$E_{(HOMO)} - E_{(LUMO)} = \Delta E \quad (3)$$

**Table 2.** Reduction of potential onset and energy levels of the different solar cells.

Extracts	$E_{\text{red}}^{\text{onset}}$ (V)	$\Delta E$ (eV)	HOMO (eV)	LUMO (eV)
CAq-Ex	- 0.45	2.08	- 6.03	- 3.95
Dcm-Ex	- 0.42	2.12	- 6.10	- 3.98
Ea-Ex	- 0.43	2.15	- 6.12	- 3.97
n-But-Ex	- 0.45	2.06	- 6.01	- 3.95

The values recorded in Table 2 were used to construct the energy level diagram for the different

*Sorghum* spp extracts (Figure 10).

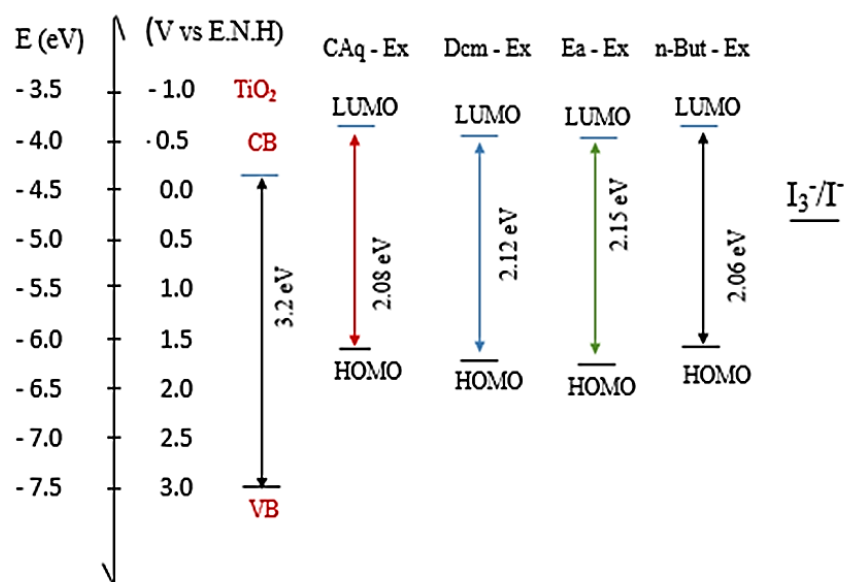


**Figure 10.** Representation of the energy level scales of the solid-state  $\text{TiO}_2$ , electrochemical extracts, and electrolyte.

The valence bands (VB) of the colored extracts are above the level of the  $\text{TiO}_2$  conduction band. Furthermore, an energy difference of more than 0.2 eV was observed between the CB of  $\text{TiO}_2$  and the VB of CAq-Ex, Dcm-Ex, Ea-Ex, and n-But-Ex, indicating that all these *Sorghum* spp-based colored extracts could inject electrons into the  $\text{TiO}_2$  conduction band. However, the energy levels of the VB obtained from Dcm-Ex and Ea-Ex were slightly lower and close to the  $\text{TiO}_2$  conduction band. This would favor better electron injection into the  $\text{TiO}_2$  conduction band for these extracts than for CAq-Ex and n-But-Ex. This is consistent with the relatively high current densities obtained by cells sensitized with the dye from Dcm-Ex and Ea-Ex. However, the HOMO energy levels of Dcm-Ex and Ea-Ex are further away from the electrolyte potential level than the HOMO energy levels of the other extracts. It would explain the relatively higher recombination rates for these extracts (Dcm-Ex and Ea-Ex) than for the n-But and CAq extracts. Similar results on *Sorghum* spp were obtained by Kallo *et al.*<sup>9</sup>, who recorded energy gap values of 2.15 eV, 2.02 eV, 2.45

eV, 2.30 eV, 2.38 eV, 2.25 eV, and 2.27 eV for the aqueous crude extract, acidified aqueous crude extract, F1 extract, F2 extract, F3 extract, F4 extract and acidified F4 extract respectively. Kumara *et al.*<sup>21</sup> also carried out similar work on natural dyes based on *Ixora* Floral (IX), obtaining energy gap values of 2.108 eV, 2.288 eV, 2.34 eV, 2.07 eV, and 3.272 eV for extracts IX, F1, F2, F3 and F4 respectively. All these extracts can then inject electrons into the  $\text{TiO}_2$  conduction band.

### 3.7. Electrochemical Impedance Spectroscopy (EIS) Characterisation

EIS was conducted to analyze the kinetic behavior of electrons in DSSC. The Nyquist plot and the electric equivalent circuit are represented in Figure 11. Three different resistances resulted from the modeling, including a series resistance ( $R_1$ ), a charge transfer resistance at the platinum/electrolyte interface ( $R_2$ ), and a charge transfer resistance at the  $\text{TiO}_2$ /dye/electrolyte interface ( $R_3$ ). These data for  $R_1$ ,  $R_2$ , and  $R_3$  are given in Table 3.



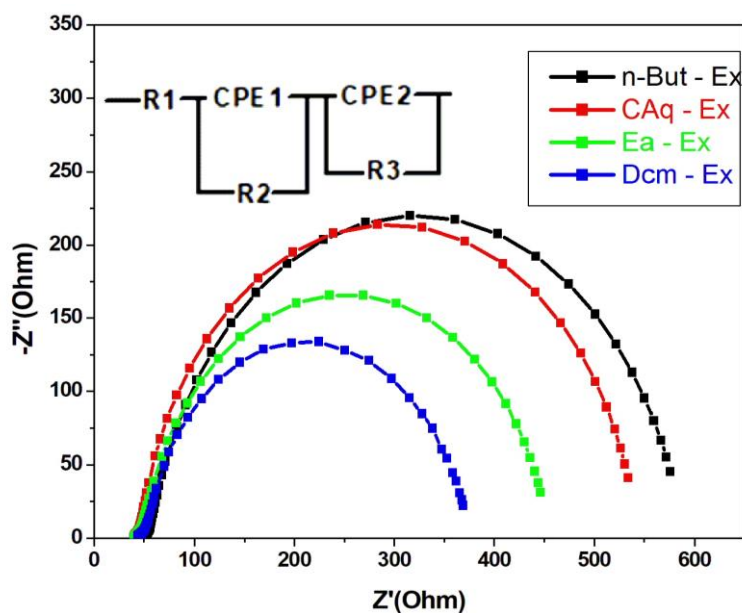


Figure 11. Nyquist plot and the electric equivalent circuit inserted.

The Bode diagram (Figure 12) shows two regions of peaks. One of these was not clearly observed. This region of semicircles is attributed to the charge transfer resistance 2 ( $R_2$ ) at the platinum/electrolyte interface corresponding to the low-frequency region in the Nyquist diagram. The other region is attributed to the charge transfer resistance 3 ( $R_3$ ) at the  $\text{TiO}_2$ /colorant/electrolyte interface (charge recombination resistance) corresponding to the

semicircles in the medium frequency region in the Nyquist diagram. The practical lifetime of electrons in  $\text{TiO}_2$  was evaluated using the Bode diagram. The latter is when an electron diffuses through the  $\text{TiO}_2$  layer before it recombines<sup>20</sup>. The effective lifetime ( $\tau_{\text{eff}}$ ) of the electrons photo-injected into the  $\text{TiO}_2$  layer is inversely proportional to the frequency ( $f_{\text{max}}$ ) of the maximum peak. The values of  $\tau_{\text{eff}}$  and  $f_{\text{max}}$  are given in Table 3.

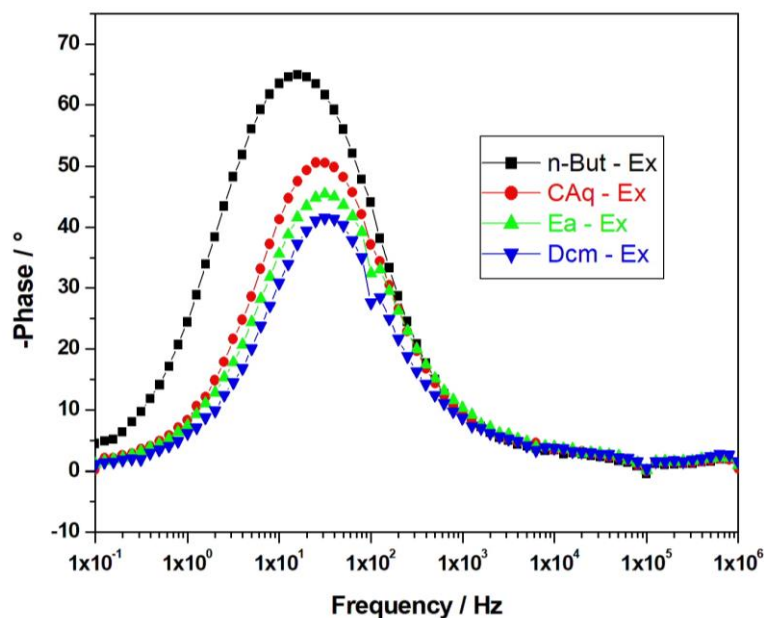


Figure 12: Bode plot.

Table 3. Electrochemical Impedance Parameters.

Extracts	$R_1$ (Ohm)	$R_2$ (Ohm)	$R_3$ (Ohm)	$f_{\text{max}}$ (Hz)	$\tau_{\text{eff}}$ (ms)
Dcm-Ex	43.45	11.30	316.59	31.577	49.575
Ea-Ex	39.72	9.72	405.98	31.577	49.575
CAq-Ex	39.37	7.31	497.06	25.081	39.377
n-But-Ex	49.48	6.66	532.27	15.824	24.843

More emphasis was put on the charge transfer resistances involving the photoanode since the platinum counter electrode and the electrolyte used in all our cells were the same. The charge recombination resistances at the TiO<sub>2</sub>/dye/electrolyte interface (R<sub>3</sub>) of the Dcm-Ex and Ea-Ex dye-sensitized solar cells were relatively lower than those of the others. This would imply higher recombination rates in the latter. These results were consistent with the lower V<sub>oc</sub> values of the Dcm-Ex and Ea-Ex dye cells compared to the others. In addition, the negative shift of the HOMO energy levels in Dcm-Ex and Ea-Ex previously demonstrated would favor recombination more, supporting the impedance results. The relatively high effective electron lifetimes of the Dcm-Ex and Ea-Ex dye cells (49.575 ms and 49.575 ms, respectively) would imply good electron injection by these dyes into the TiO<sub>2</sub>. These results are consistent with the high current density values previously observed in the photovoltaic parameters of Dcm-Ex and Ea-Ex dye cells.

Furthermore, the low electron recombination resistances observed in the latter would imply an increase in the current density (J<sub>sc</sub>), which would lead to high conversion efficiencies<sup>21</sup>, as Luo *et al.*<sup>22</sup> observed in their work. These authors investigated DSSCs with extracts of *Canna indica* L., *Salvia splendens*, cowberry, and *Solanum nigrum* L. as sensitizers. They found a significantly high resistance of 27902 Ohm at the TiO<sub>2</sub>/dye/electrolyte interface of the cell sensitized with cowberry dye, which decreased both the current density and the solar energy conversion efficiency. In our work, the impedance results (lower recombination resistances and longer electron lifetimes) are in line with the best conversion rates obtained by the Dcm-Ex and Ea-Ex cells within the photovoltaic parameters previously obtained. This conclusion can be found in the work of authors such as Ammar *et al.*<sup>10</sup>, who worked on dye solar cells sensitized with spinach, onion, and red cabbage extracts. They observed that the charge transfer resistances for the three extract dyes were 126.3, 371.3, and 430 Ohm, respectively, and they concluded that spinach dye has high efficiency due to its lower charge transfer resistance and longer carrier lifetime (20.98 ms).

#### 4. Conclusion

Natural dyes mainly composed of anthocyanin extracted from *Sorghum spp* have been employed as DSSC sensitizers. A liquid-liquid separation technique of the aqueous crude extract was performed to improve the conversion rate with organic solvents of increasing polarity, such as dichloromethane, ethyl acetate, and n-butanol. Among the colored extracts, dichloromethane and ethyl acetate extracts recorded the best conversion efficiencies  $\eta = 0.19\%$  and  $\eta = 0.18\%$ , respectively. These cells also exhibited the lowest charge transfer

resistances (R<sub>3</sub>) at the TiO<sub>2</sub>/dye/electrolyte interface (316.59 Ohm, 497.06 Ohm), high recombination rates, low V<sub>oc</sub> values (412 mV and 420 mV, respectively), high current densities (1.079 mA.cm<sup>-2</sup> and 0.83 mA.cm<sup>-2</sup>, respectively), and the most extended electron lifetime in TiO<sub>2</sub> (49.575 ms). All these results indicate good electron injection and efficient transfer, enabling these cells to convert light more effectively. In conclusion, this study helps to interpret the electronic exchanges and photovoltaic performances in DSSCs.

#### 5. Acknowledgements

The authors are grateful to The World Academy of Sciences (TWAS, Grant No. 19-160 RG/CHE/AF/AC\_I - FR3240310170) support.

#### References

- 1- J. Wang, W. Azam, Natural resource scarcity, fossil fuel energy consumption, and total greenhouse gas emissions in top emitting countries, *Geosci. Front.*, **2024**, 15, 101757. <https://doi.org/10.1016/j.gsf.2023.101757>
- 2- S. A. Siddique, B. Ali, M. B. A. Siddique, A. Rauf, R. Hussain, M. A. Ali, T. Mahmood, S. Altaf, A. Rauf, S. J. F. Alanazi, A. M. Al-Mohaimeed, X. Liu, M. Arshad, Discovery of pyrrole-triphenylamine based novel organic sensitizers for dye-sensitized solar cells: A first principal study, *Mater. Sci. Semicond. Process.*, **2024**, 174, 108173-108173. <https://doi.org/10.1016/j.mssp.2024.108173>
- 3- O. I. Francis, A. Ikenna, Review of dye-sensitized solar cell (DSSCs) development. *Nat. Sci.* **2021**, 13, 496–509. <https://doi.org/10.4236/ns.2021.1312043>
- 4- A. S. R. Bati, Y. L. Zhong, P. L. Burn, M. K. Nazeeruddin, P. E. Shaw, M. Batmunkh, Next-generation applications for integrated perovskite solar cells, *Commun. Mater.*, **2023**, 4, 1-24. <https://doi.org/10.1038/s43246-022-00325-4>
- 5- S. A. Mahadik, H. M. Pathan, S. Salunke-Gawali, An Overview of Metal Complexes, Metal-Free and Natural Photosensitizers in Dye-Sensitized Solar Cells, *ES Energy & Environ.*, **2024**, 24, 1078. <https://doi.org/10.30919/esee1078>
- 6- G. F. C. Mejica, Y. Unpaprom, R. Ramaraj, Fabrication and performance evaluation of dye-sensitized solar cell integrated with natural dye from *Strobilanthes cusia* under different counter-electrode materials, *Appl. Nanosci.*, **2021**, 13, 1073-1083. <https://doi.org/10.1007/s13204-021-01853-0>
- 7- A. Triyanto, N. A. Ali, H. Salleh, J. Setiawan, N. I. Yatim, Development of natural dye photosensitizers for dye-sensitized solar cells: a review, *Environ. Sci. Pollut. Res.*, **2024**, 31,

- 31679-31690. <https://doi.org/10.1007/s11356-024-33360-4>
- 8- H. Zhou, L. Wu, Y. Gao, T. Ma, Dye-sensitized solar cells using 20 natural dyes as sensitizers, *J. Photochem. Photobiol., A*, **2011**, 219, 188–194. <https://doi.org/10.1016/j.jphotochem.2011.02.008>
- 9- M. S. Kallo, A. A. Mahamane, S. A. Boulhassance, R. Adamou, Dye-sensitized solar cell using natural anthocyanin dyes extracted from Sorghum Spp (Poaceae) sheaths, *Journal of Applied Chemistry (IOSR-JAC)*, **2021**, 14, 01-09. <https://doi.org/10.9790/5736-1409010109>
- 10- A. M. Ammar, H. S. H. Mohamed, M. M. K. Yousef, G. M. Abdel-Hafez, A. S. Hassanien, A. S. G. Khalil, Dye-Sensitized Solar Cells (DSSCs) Based on Extracted Natural Dyes, *J. Nanom.*, **2019**, 1-10. <https://doi.org/10.1155/2019/1867271>
- 11- M. D. A. Sanda, M. Badu, J. A. M. Awudza, N. O. Boadi, Development of TiO<sub>2</sub>-based dye-sensitized solar cells using natural dyes extracted from some plant-based materials, *Journal of Chemistry International*, **2021**, 7, 9-20. <https://doi.org/10.5281/zenodo.4018012>
- 12- S. Alhorani, S. Kumar, M. Genwa, P. L. Meena, Performance of dye-sensitized solar cells extracted dye from wood apple leaves, *J. Phys. Commun.*, **2022**, 6, 085012. <https://doi.org/10.1088/2399-6528/ac8785>
- 13- M. A. M. Al-Alwani, A. B. Mohamad, A. A. H. Kadhum, N. A. Ludin, Effect of solvent on the extraction of natural pigments and adsorption onto TiO<sub>2</sub> for dye sensitized solar cell applications, *Spectrochim. Acta A Mol. Biomol. Spectrosc.*, **2015**, 138, 130-137. <http://dx.doi.org/10.1016/j.saa.2014.11.018>
- 14- G. F. C. Mejica, Y. Unpaprom, R. Ramaraj, Fabrication and performance evaluation of dye-sensitized solar cell integrated with natural dye from *Strobilanthes cusia* under different counter-electrode materials, *RSC Adv.*, **2021**, 5, 68929-68938. <https://doi.org/10.1007/s13204-021-01853-0>
- 15- A. Lim, N. T. R. N. Kumara, A. L. Tan, A. H. Mirza, R. L. N. Chandrakanthi, M. I. Petra, L. C. Ming, G. K. R. Senadeera, P. Ekanayake, Potential natural sensitizers extracted from the skin of *Canarium odontophyllum* fruits for dye-sensitized solar cells, *Spectrochim. Acta A Mol. Biomol. Spectrosc.*, **2015**, 138, 596-602. <http://dx.doi.org/10.1016/j.saa.2014.11.102>
- 16- E. P. Mukhokosi, M. Maaza, M. Tibenkana, N. L. Botha, L. Namanya, I. G. Madiba, M. Okullo, Optical absorption and photoluminescence properties of Cucurbita maxima dye adsorption on TiO<sub>2</sub> nanoparticles, *Mater. Res. Express*, **2023**, 10, 046203. <https://doi.org/10.1088/2053-1591/acce91>
- 17- E. C. Prima, H. S. Nugroho, G. Refantero, C. Panatarani, B. Yulianto, Performance of the dye-sensitized quasi-solid state solar cell with combined anthocyanin-ruthenium photosensitizer, *RSC Adv.*, **2020**, 10, 36873-36886. <https://doi.org/10.1039/D0RA06550A>
- 18- E. V. Verbitskiy, E. M. Cheprakova, J. O. Subbotina, A. V. Schepochkin, P. A. Slepukhin, G. L. Rusinov, V. I. Minkin, Synthesis, spectral and electrochemical properties of pyrimidine-containing dyes as photosensitizers for dye-sensitized solar cells, *Dyes and Pigm.*, **2014**, 100, 201-214. <https://doi.org/10.1016/j.dyepig.2013.09.006>
- 19- L. Leonat, G. Sbarcea, I. V. Branzoi, Cyclic voltammetry for energy levels estimation of organic materials, *UPB Sci. Bull. Ser. B*, **2013**, 75, 111-118. [https://www.scientificbulletin.upb.ro/rev\\_docs\\_arhiva/rezdd1\\_869282.pdf](https://www.scientificbulletin.upb.ro/rev_docs_arhiva/rezdd1_869282.pdf)
- 20- N. E. Safie, N. A. Ludin, N. H. Hamid, P. M. Tahir, M. A. M. Teridi, S. Sepeai, K. Sopian, Electron transport studies of dye sensitized solar cells based on natural sensitizer extracted from rengas (*Gluta spp.*) and mengkulang (*Heritiera elata*) wood, *BioResources*, **2017**, 12, 9227-9243. <https://doi.org/10.15376/bioresources.12.4.9227-9243>
- 21- N. T. R. N. Kumara, M. Petrović, D. S. U. Peiris, Y. A. Marie, C. Vijila, M. I. Petra, P. Ekanayake, Efficiency enhancement of *Ixora floral* dye sensitized solar cell by diminishing the pigments interactions, *Sol. Energy.*, **2015**, 117, 36-45. <https://doi.org/10.1016/j.solener.2015.04.019>
- 22- P. Luo, H. Niu, G. Zheng, X. Bai, M. Zhang, W. Wang, From salmon pink to blue natural sensitizers for solar cells: *Canna indica* L., *Salvia splendens*, *cowberry* and *Solanum nigrum* L. *Spectrochim. Acta Part A Mol. Biomol. Spectrosc.*, **2009**, 74, 936-942. <https://doi.org/10.1016/j.saa.2009.08.039>